

This article was downloaded by:

On: 23 January 2011

Access details: *Access Details: Free Access*

Publisher *Taylor & Francis*

Informa Ltd Registered in England and Wales Registered Number: 1072954 Registered office: Mortimer House, 37-41 Mortimer Street, London W1T 3JH, UK



Journal of Coordination Chemistry

Publication details, including instructions for authors and subscription information:

<http://www.informaworld.com/smpp/title~content=t713455674>

DISTINCTIVE COORDINATION CHEMISTRY AND BIOLOGICAL RELEVANCE OF COMPLEXES WITH MACROCYCLIC OXO POLYAMINES

Eiichi Kimura^a

^a Department of Medicinal Chemistry, Hiroshima University School of Medicine, Kasumi, Hiroshima, Japan

To cite this Article Kimura, Eiichi(1986) 'DISTINCTIVE COORDINATION CHEMISTRY AND BIOLOGICAL RELEVANCE OF COMPLEXES WITH MACROCYCLIC OXO POLYAMINES', *Journal of Coordination Chemistry*, 15: 1, 1 – 28

To link to this Article: DOI: 10.1080/00958978608075853

URL: <http://dx.doi.org/10.1080/00958978608075853>

PLEASE SCROLL DOWN FOR ARTICLE

Full terms and conditions of use: <http://www.informaworld.com/terms-and-conditions-of-access.pdf>

This article may be used for research, teaching and private study purposes. Any substantial or systematic reproduction, re-distribution, re-selling, loan or sub-licensing, systematic supply or distribution in any form to anyone is expressly forbidden.

The publisher does not give any warranty express or implied or make any representation that the contents will be complete or accurate or up to date. The accuracy of any instructions, formulae and drug doses should be independently verified with primary sources. The publisher shall not be liable for any loss, actions, claims, proceedings, demand or costs or damages whatsoever or howsoever caused arising directly or indirectly in connection with or arising out of the use of this material.

DISTINCTIVE COORDINATION CHEMISTRY AND BIOLOGICAL RELEVANCE OF COMPLEXES WITH MACROCYCLIC OXO POLYAMINES

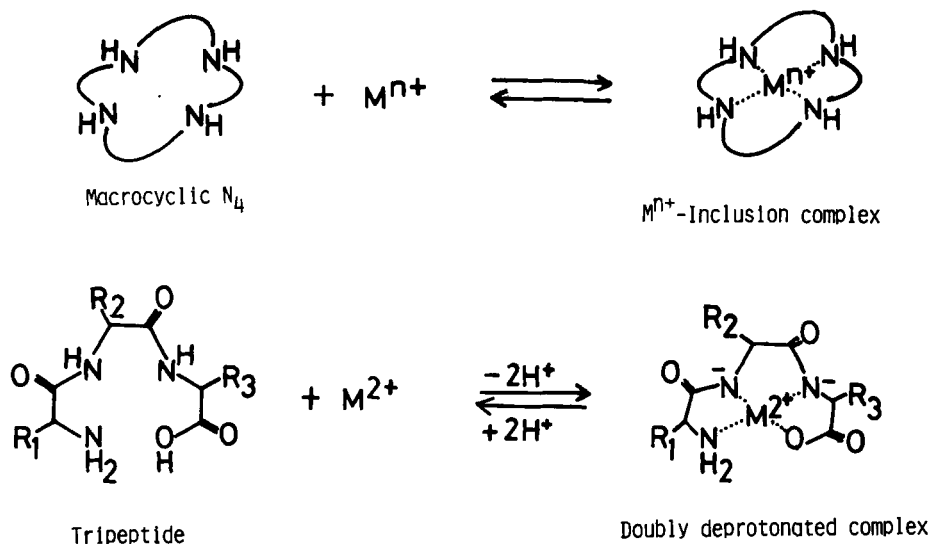
EIICHI KIMURA

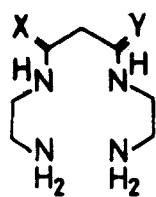
Department of Medicinal Chemistry, Hiroshima University School of Medicine, Kasumi, Hiroshima 734, Japan

Replacement of amine with amide groups in macrocyclic polyamines yields a novel series of oxo polyamine ligands which are the hybrids of macrocyclic polyamines and linear oligopeptides. Due to the involvement of imide anions in coordination, their ligand fields are stronger compared to those of macrocyclic counterparts. One consequence is stabilization of unusual oxidation states Cu^{III} and Ni^{III} .

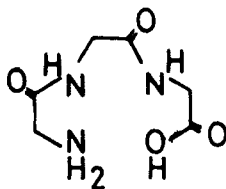
1. INTRODUCTION

Macrocyclic oxo polyamines depicted in Figure 1 (with abbreviated names) are unique metal chelators recently discovered and developed by us.¹⁻³ Their structures bear the dual features of macrocyclic polyamines and oligopeptides. The macrocyclic ligands offer unusually high ligand field strengths to those metal ions having the ionic diameters matched to the macrocyclic cavities and the resulting complexes are extremely stable thermodynamically and kinetically.^{4,5} As polyamine donor ligands, they have affinities for a broad range of heavy metal ions and transition metal ions. Certain macrocyclic polyamines can enclose alkali metal ions and alkaline earth metal ions.^{6,7} In contrast, oligopeptides such as triglycine and tetraglycine complex with a very limited number of metal ions Cu^{2+} , Ni^{2+} , Co^{2+} , Pd^{2+} and the complex dissociation is easy and fast.^{8,9} Their structural features for biological significance are well recognized.

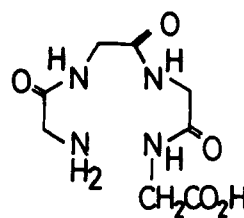




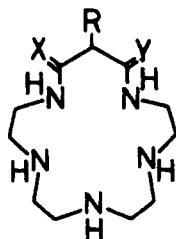
$X=Y=H_2$: 2,3,2-tet
 $X=Y=O$: dioxo [2,3,2] tet



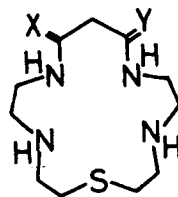
triglycine



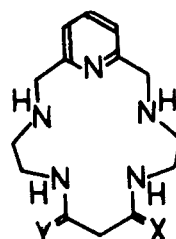
tetraglycine



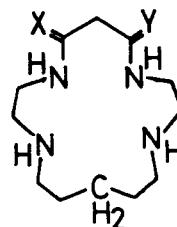
$X=Y=H_2$: [16]ane N_5
 $X=H_2, Y=O$: monooxo[16]ane N_5
 $X=Y=O$: dioxo[16]ane N_5



$X=Y=H_2$: [16]ane N_4S
 $X=Y=O$: dioxo[16]ane N_4S

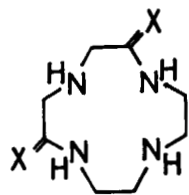


$X=Y=H_2$: pyo[16]ane N_5
 $X=Y=O$: pyodioxo[16]ane N_5

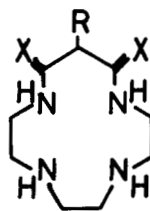


$X=Y=H_2$: [16]ane $N_4(CH_2)$
 $X=Y=O$: dioxo[16]ane $N_4(CH_2)$

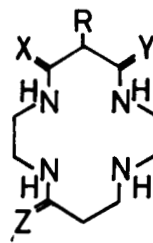
FIGURE 1 Structure and abbreviation of oxo polyamine ligands described in this review.



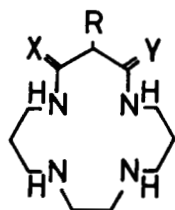
$X=H_2$: [12]ane N_4
 $X=O$: dioxo [12]ane N_4



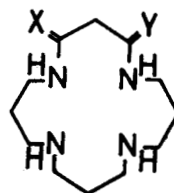
$X=H_2$: [13]ane N_4
 $X=O$: dioxo [13]ane N_4



$X=Y=Z=H_2$: [14]ane N_4
 $X=O, Y=Z=H_2$: monooxo [14]ane N_4
 $X=Y=O, Z=H_2$: dioxo [14]ane N_4
 $X=Y=Z=O$: trioxo [14]ane N_4



$X=Y=Z=H_2$: [15]ane N_4
 $X=Y=O$: dioxo [15]ane N_4



$X=Y=H_2$: [16]ane N_4
 $X=Y=O$: dioxo [16]ane N_4

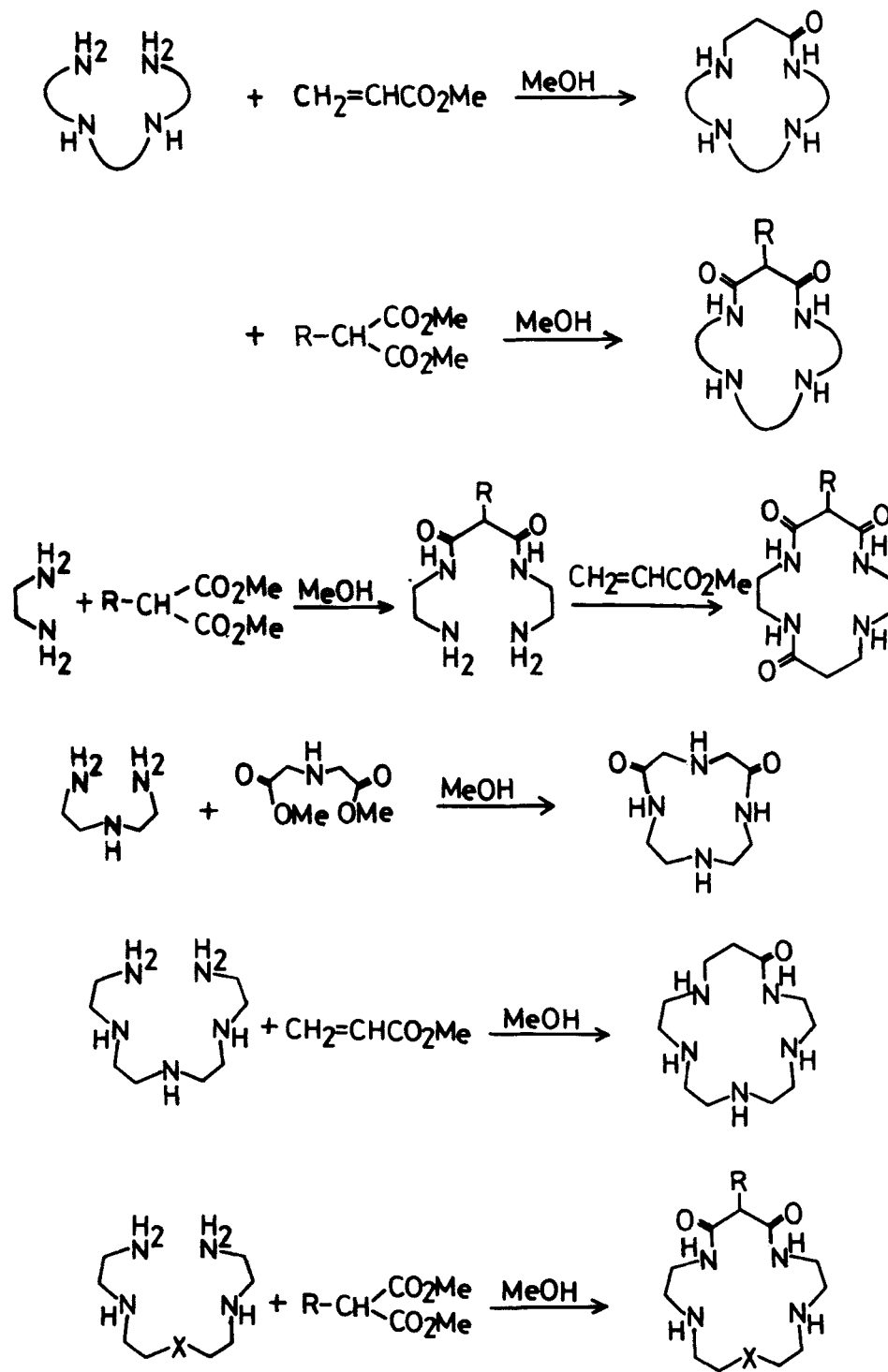
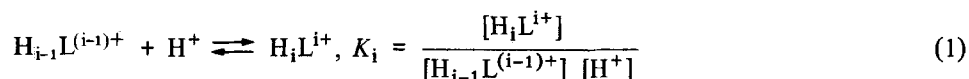


FIGURE 2 General scheme for synthesis of macrocyclic oxo polyamines.

In 1979 we designed a combination of macrocyclic tetraamines and oligopeptides to explore a new ligand system.¹ We chose to work first with the macrocyclic dioxo tetraamines dioxo(13)-(16)aneN₄ that had already been prepared by Tabushi et al. from linear tetraamines and malonate esters as synthetic intermediates for macrocyclic saturated tetraamines.¹⁰ Our first complexation study was very successful, showing the dioxo(13)-(15)aneN₄ to possess the anticipated properties.¹ Subsequently we have modified and synthesized a wider variety of oxo polyamines and expanded the scope of our studies. We have now found quite a few unexpected novel and unique features in them, which have biological relevance as well as being of interest from the point of view of coordination chemistry. The general procedure for preparation of oxo polyamines is outlined in Figure 2. Interested readers may find the details in the references to be cited in the subsequent sections.

2. GENERAL PROPERTIES OF OXO POLYAMINE LIGANDS

Incorporation of one, two or three carbonyl groups at the α -carbons and tetraamines converts the tetraamines into triamine, diamine, or monoamine bases, respectively, and furthermore lowers the basicities of the remaining amine groups in that order as can be seen by comparing the first mixed protonation constants $\log K_1$ (Eq. (1))



for macrocyclic tetraamines with or without oxo functions (Table I). This effect is greatest in the smallest cyclic system (12)aneN₄ and least in the open chain or the largest cyclic (15)aneN₄. These protonation trends affect kinetic behavior in the complexation reactions. The complexation of N^{2+} with dioxo(13)-(15)aneN₄ is apparently faster than with the corresponding oxo-free[13]-[15]aneN₄, since the more unprotonated species are available for the dioxo system at the comparable pH conditions. At a given pH (e.g. in acetate buffer), the observed rate of Cu^{2+} complexation is about ten times faster with dioxo(13)aneN₄ than with the dioxo(14)aneN₄ because the competitive proton affinities are lower for dioxo(13)aneN₄.

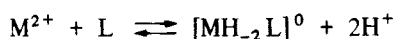
TABLE I
Mixed Protonation Constants for Oxo-free Polyamine and Oxo Polyamine Ligands at 25°C and
 $I = 0.2 \text{ M}^{1,3,26,30}$

Ligand	$\log K_1$	$\log K_2$	$\log K_3$	$\log K_4$	$\log K_5$
2,3,2-tet	10.25	9.50			
dioxo 2,3,2-tet	9.08	8.82			
(12)aneN ₄	10.70	9.7	1.7	0.9	
dioxo(12)aneN ₄	7.60	4.40			
(13)aneN ₄	11.10	10.10	1.7	1	
dioxo(13)aneN ₄	9.05	3.82			
(14)aneN ₄	11.50	10.30	1.6	0.9	
monooxo(14)aneN ₄	10.24	6.9	2.9		
dioxo(14)aneN ₄	9.57	5.97			
trioxo(14)aneN ₄	8.38				
(15)aneN ₄	11.20	10.10	<2	<2	
dioxo(15)aneN ₄	9.40	6.52			
(16)aneN ₅	10.64	9.49	7.28	1.7	1.5
monooxo(16)aneN ₅ ^a	9.68	8.65	5.71	<2	
dioxo(16)aneN ₅ ^a	9.01	8.69	<2		

^aAt 35°C

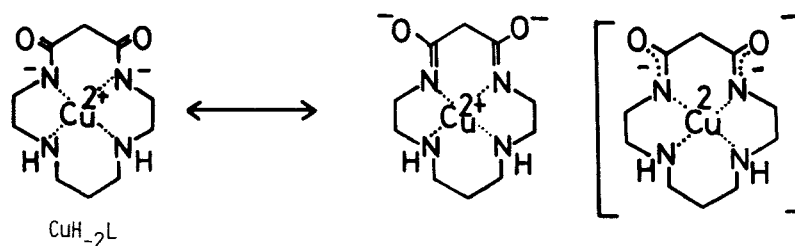
Potentiometric titration of the diprotonated dioxo tetraamine ligands clearly shows the dissociation of two more protons in the presence of certain bivalent metal ions to indicate the complexation with simultaneous dissociation of the two amide protons (Figure 3). The successful metal ions are Cu^{2+} ,¹ Ni^{2+} ,³ or Co^{2+} ,¹¹ all of which have been reported to favor square planar coordination and form stable 1:1 complexes with deprotonated oligopeptides at varying pH (normally 4–6 for Cu, 7–8 for Ni, 10–11 for Co).⁹ With Zn^{2+} , Cd^{2+} or Pb^{2+} the dioxo ligands have little interaction.¹ Thus, the dioxo tetraamines are more selective transition metal chelating agents. The complexation of Cu^{2+} goes to completion at $\text{pH} < 5$ with dioxo(13)- and dioxo(14)ane N_4 and at $\text{pH} 7$ with dioxo(15)ane N_4 and dioxo 2,3,2-tet, which are far below the buffer pH of peptide in the presence of Cu^{2+} (see Fig. 3). Ni^{2+} complexes with dioxo(13)- and (14)ane N_4 below $\text{pH} 6$ and with dioxo(15)ane N_4 below $\text{pH} 8$. Co^{2+} chelates with dioxo(13)- at $\text{pH} < 8.5$, and (14)ane N_4 (at $\text{pH} < 7.8$), but not with dioxo(15)ane N_4 at measurable pH.

The titration data of dioxo(13)–(15)ane N_4 (L) for buffer pH regions in the presence of M^{2+} are all in best agreement with the formation of MH_{-2}L complexes as expressed by Eq. (2).



$$K_{\text{MH}_{-2}\text{L}} = \frac{[\text{MH}_{-2}\text{L}] [\text{H}^+]^2}{[\text{M}^{2+}] [\text{L}]} \quad (2)$$

The formula MH_{-2}L is consistent with coordination of the two amide nitrogens with displacement of the amide protons. Presence of non deprotonated $(\text{ML})^{2+}$ or singly deprotonated $(\text{MH}_{-1}\text{L})^+$ is unlikely. The determined $K_{\text{MH}_{-2}\text{L}}$ values are summarized in Table II. The copper(II) complex of dioxo(14)ane N_4 , CuH_{-2}L , is isolable as violet crystals from aqueous solution. Its IR spectrum (KBr) shows $\nu_{\text{C}=\theta}$ at 1580 cm^{-1} which is far lower than 1655 cm^{-1} of the free ligand, indicating the contribution of the anion-delocalized structure, as is the case for peptide complexes.⁹ It is considered that the C–N[−] (trigonal) distances are shorter than the C–N (tetrahedral) distances and hence the ring cavity of the dioxo macrocycles is narrower with respect to the oxo-free homologues.



Palladium(II) also yields a colorless, crystalline 1:1 complex, PdH_{-2}L , with dioxo(14)ane N_4 , which displays a similar value of $\nu_{\text{C}=\theta}$.

The d–d absorption spectra for the Cu^{2+} -dioxo(13)–(15)ane N_4 complexes (505–520 nm, see Table 2) occur in the vicinity of those for the square planar dioxo 2,3,2-tet complex (515 nm)¹² and tetraglycine complex (515 nm),^{8,9} lending a support to an assignment of a similar coordination environment about Cu^{2+} ion. The narrow range of the visible

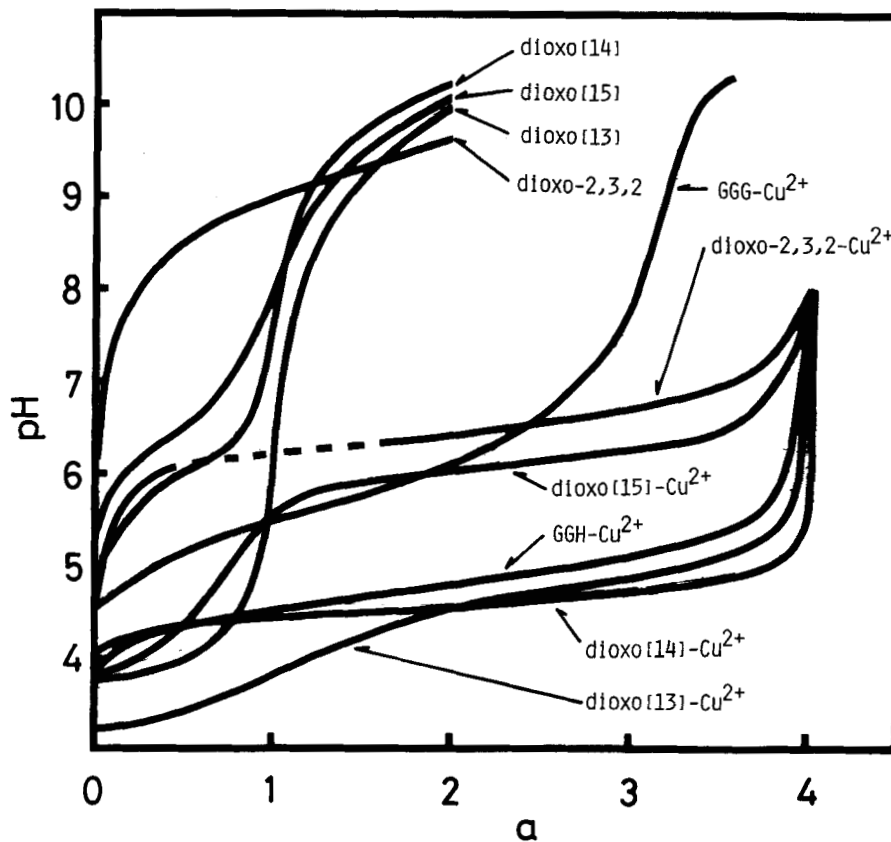


FIGURE 3 Potentiometric titration curves of dioxo(13)-(15)ane $N_4 \cdot 2HClO_4$, dioxo 2,3,2-tet $\cdot 2HClO_4$ with and without equimolar Cu^{2+} . The titration curves of triglycine (GGG) and GlyGlyHis (GGH) with equimolar Cu^{2+} are also shown. α is NaOH titration point.

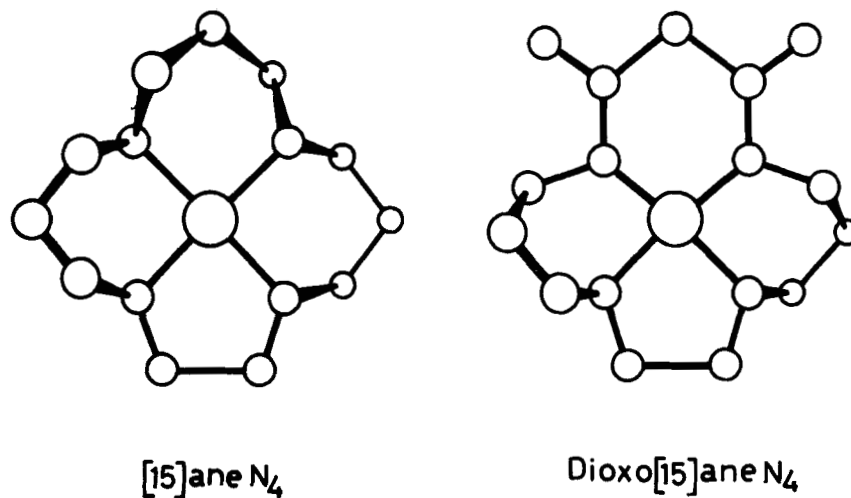


FIGURE 4 Comparison of molecular models for square-planar complexes of (15)ane N_4 and doubly deprotonated dioxo(15)ane N_4 .

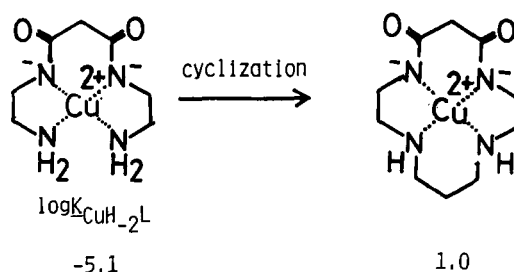
TABLE II
Some Properties of 1:1 Metal Complexes at $I = 0.2$ M and 25°C (Cu^{2+}) or 35°C (Ni^{2+}), 1,3,36,30

Metal ion	Ligand(L)	Complex Formula	$\log K_{\text{ML}_2\text{L}^2/\text{M}}$ or $\log K_{\text{ML}_2\text{L}^2/\text{M}^{2+}}$	$\lambda_{\text{max}}/\text{nm}$ ($\epsilon/\text{M}^{-1}\text{cm}^{-1}$)	$E_{1/2}$ for $\text{M}^{\text{III/II}}/\text{V}$ vs SCE
Copper(II)	dioxo(12)aneN ₄	(CuH ₂ L)	-9.2	620(150)	0.42
	(12)aneN ₄	(CuL) ₂ ⁺	24.8	600	
	dioxo(13)aneN ₄	(CuH ₂ L)	-2.2	520(100)	0.56
	(13)aneN ₄	(CuL) ₂ ⁺	29.1	550	
	dioxo(14)aneN ₄	(CuH ₂ L)	1.0	505(100)	0.64
	(14)aneN ₄	(CuL) ₂ ⁺	27.2 ^a	505	
	dioxo(15)aneN ₄	(CuH ₂ L)	-4.5	520(100)	0.69
	(15)aneN ₄	(CuL) ₂ ⁺	24.4	570	
	dioxo(16)aneN ₄	(CuH ₂ L)	-10.1		0.93
	dioxo2,3,2-tet	(CuH ₂ L)	-5.1	515(100)	0.70
	2,3,2-tet	(CuL) ₂ ⁺	23.9		
	GlyGlyGly	(CuH ₂ L)	-6.5	555(100)	0.67
	GlyGlyHis	(CuH ₂ L)	-2.1	530	0.38
	GlyGlyGlyGly	(CuH ₂ L)		515	0.62
	Nickel(II)	dioxo(12)aneN ₄	(NiH ₂ L)	-12.6	465(100)
(12)aneN ₄		low spin NiL ₂ ⁺		430	
dioxo(13)aneN ₄		(NiH ₂ L)	-6.05	412(110)	0.92
(13)aneN ₄		low spin NiL ₂ ⁺		425	irreversible
dioxo(14)aneN ₄		(NiH ₂ L)	-5.15	460(100)	0.80
(14)aneN ₄		low spin NiL ₂ ⁺		444	0.50
dioxo(15)aneN ₄		(NiH ₂ L)	-8.92	450(100)	0.62
(15)aneN ₄		low spin NiL ₂ ⁺		466	0.77
dioxo(16)aneN ₄		ppt			
dioxo2,3,2-tet		(NiH ₂ L)	9.86	450(80)	irreversible
2,3,2-tet		low spin NiL ₂ ⁺		445	
GlyGlyGly		(NiH ₂ L)	-12.8	430	0.60
GlyGlyGlyGly		(NiH ₂ L)		412	0.54
dioxo(13)aneN ₄		(CoH ₂ L)	-12.43		-0.35
(13)aneN ₄		(CoL) ₂ ⁺	14.28		
dioxo(14)aneN ₄	(CoH ₂ L)	-8.44		-0.31	
(14)aneN ₄	(CoL) ₂ ⁺	12.71		-0.40	

^aA composite of two isomers

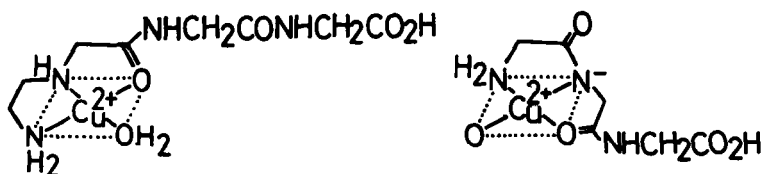
absorption maxima among the 13–15 membered dioxo homologues is in contrast to the wide range of the oxo-free counterparts: λ_{\max} 550 nm ((13)aneN₄), 505 nm ((14)aneN₄), and 570 nm ((15)aneN₄). These oxo-free macrocycles tend to take coplanar coordination,^{13,14} and the coplanar (14)aneN₄ is considered to fit best with Cu²⁺.¹⁵ The ligand field strengths of the 14-membered N₄ macrocycles are nearly the same with or without oxo groups, since they exhibit the same λ_{\max} value of 505 nm. The smaller deviations from this value for the dioxo(13)- and dioxo(15)aneN₄ are evidence for a more coplanar character of the dioxo N₄ coordinate environments. Especially, in comparison of (15)aneN₄¹⁴ and dioxo(15)aneN₄ (Figure 4), the effect of the two trigonally sp²-hybridized nitrogens will become clear on the attainment of coplanar N₄. In the dioxo system, the two propylenediamine chelates are rendered more easily and properly twisted, and the two sp³ N's can take unstrained tetrahedral geometry. The two imides similarly should enforce the planarity of the 13-membered N₄ formed by the 2,2,2-tet (trien)chelate.

The cyclization effect and the macrocyclic ring size effect, both the effects which were already well established for Cu²⁺ oxo-free tetraamine complexes,^{16–20} are also prominent in the dioxo tetraamine series. Comparison of log K_{CuH₂L} values (Table II) shows a macrocyclic effect of six orders of magnitude (*cf.* dioxo(14)aneN₄ vs. dioxo 2,3,2,-tet). The most stable complex forms with the 14-membered ligand because its cavity provides the best fit to Cu²⁺. The greatest d–d transition energy (505 nm) of this complex indicates the evidence that it has the greatest in-plane ligand field strength.



3. COMPARISON WITH TRIPEPTIDE LIGANDS

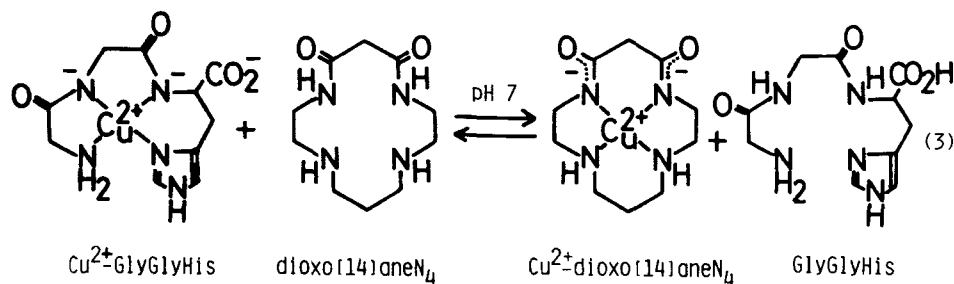
Copper(II) successively (as pH is raised) displaces peptide protons in complexation with tri- and tetrapeptides. Nickel(II), on the other hand, does so almost simultaneously. Thus, with triglycine, CuL, CuH_{−1}L, and the final CuH_{−2}L are formed and their proportion varies with the solution pH, while NiH_{−2}L is the only measurable complex species.⁹ At lower pH, the undeprotonated CuL species is predominant and at higher pH, the proportion of doubly deprotonated MH_{−2}L increases. The structures of CuL and CuH_{−1}L are considered as follows:



Adoption of such structures possessing the amide oxygen coordination (instead of the amide nitrogen) is impossible with the dioxo(13)-(15)aneN₄ which have little conformational flexibility. The pH titration results rule out the occurrence of CuL, NiL, CoL, CuH₋₁L, NiH₋₁L, and CoH₋₁L.¹⁻³ a fact also disproving di- or tridentate ligation property of dioxo(13)-(15)aneN₄. The interaction of M²⁺ with the dioxo macrocycles occurs initially at the two secondary amines, followed by immediate displacement for the two amide hydrogens, finishing in the stable M²⁺-inclusion complexes. This synchronized action should be characteristic of the macrocyclic tetraamines having appropriate holes. Its driving force or the increased acidity of the amide hydrogens obviously derives from facile encapsulation into the macrocyclic cavities.

In acidic pH regions, the complexation with M²⁺ occurs more favorably for the macrocyclic ligands than for linear homologues. This is typically shown by calculation of the degree of dissociation at [Cu²⁺] = [L] = 10⁻³ M and pH 5.50 using the protonation constants and the reported K_{CuH_{-n}L} values: 7% (dioxo(13)aneN₄), 1% (dioxo(14)aneN₄), 16% (dioxo(15)aneN₄), 92% (dioxo 2.3.2-tet), 51% (triglycine), and 13% (GlyGlyHis).¹ It is to be noted that the peptide complexes include a mixture of (CuL), (CuH₋₁L) and (CuH₋₂L), while the dioxo complexes consist only of (CuH₋₂L).

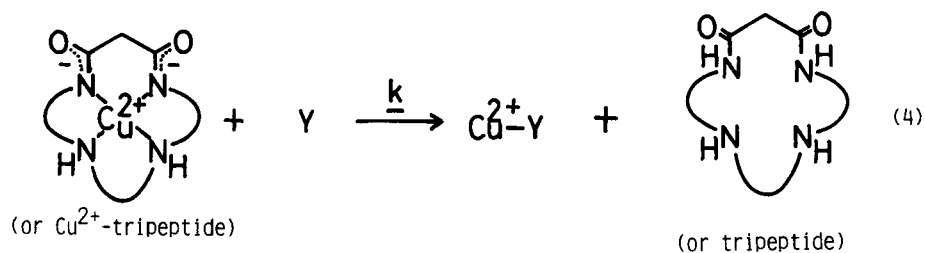
Calculations show that mixing equimolar [metal] and [ligand] solutions at pH 7 yields the doubly deprotonated CuH₋₂L complexes in virtually 100% for dioxo(14)aneN₄ and GlyGlyHis, where one would predict higher stability of the former complex based on the relative K_{CuH₋₂L} values. The equilibrium constant for Eq. (3) is calculated to be about 10^{2.2}.



The overwhelming shift to the right in Eq. (3) is experimentally demonstrated by the exclusive occurrence of visible absorption of Cu²⁺-dioxo(14)aneN₄ complex in equimolar GlyGlyHis at pH 7.0 (phosphate buffer). Since GlyGlyHis is a molecule designed to mimic the copper(II)-specific transport site of serum albumin,^{21,22} the macrocyclic dioxotetraamines may be interesting as a drug to remove excess copper(II) ion from the body.

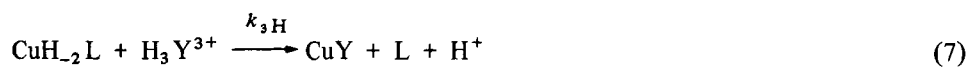
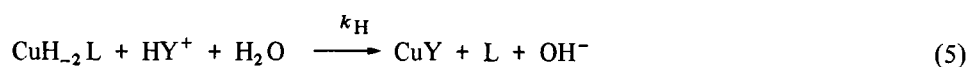
4. KINETICS OF LIGAND-DISPLACEMENT OF Cu²⁺-DIOXO(13)-(15)aneN₄

The higher thermodynamic stability of macrocyclic dioxo complexes with respect to tripeptides is associated with kinetic inertness toward the ligand dissociation. This is well demonstrated in the ligand-displacement kinetics for Eq. (4).²

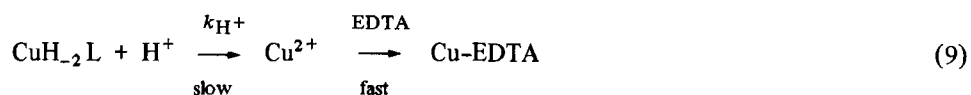
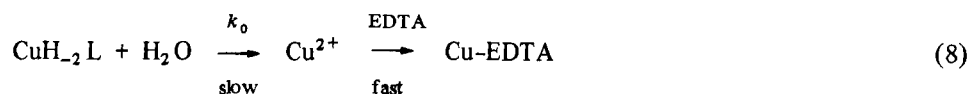


The rates at varying pH were analyzed as follows.

For trien (Y) reactions, three reactions (5)–(7) occur at the same time.



For EDTA (Y) reactions, three pathways (8)–(10) lead to the final product.



All the specific rate constants are summarized in Table III.

Although triglycine and dioxo 2,3,2-tet assume similar square-planar coordination, they differ significantly in their kinetic behavior to trien. The observed second-order rate constants at a given pH are much smaller with dioxo 2,3,2-tet, and as the solution pH decreases, the replacement of triglycine becomes slower while the opposite is true with dioxo 2,3,2-tet. The behaviour of dioxo 2,3,2-tet is similar to GlyGlyHis,² where an intermolecular proton transfer from the protonated trien to the deprotonated amide sites is required prior to or during the rate-determining step for the breakage of a copper-imide bond. On the other hand, the replacement of triglycine by trien is considered to start with a direct nucleophilic substitution of the terminal carboxylate group by the amine. The inert nature of the Cu-terminal N bonding (in dioxo 2,3,2-tet) relative to the labile Cu-carboxylate bonding (in triglycine) is responsible for the different reaction mechanisms.

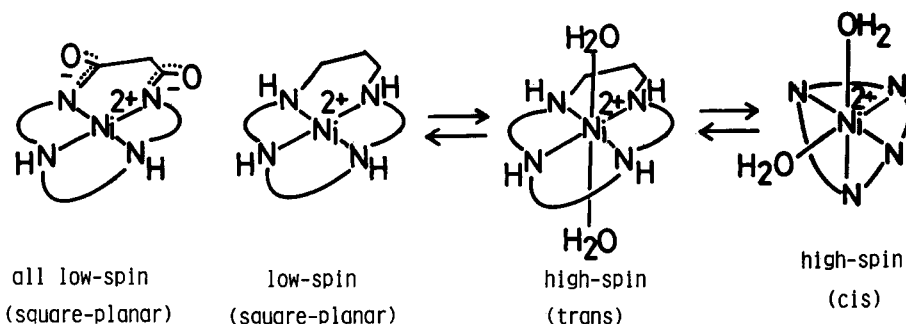
TABLE III
Rate Constants (all in $\text{mol}^{-1}\text{dm}^3\text{ s}^{-1}$ except for k_{O} in s^{-1}) for reaction of 2,2,2-tet and EDTA with $(\text{CuH}_2\text{X})_2^2$

	X					
	dioxo2,3,2-tet	dioxo(13)aneN ₄	dioxo(14)aneN ₄	dioxo(15)aneN ₄	Trigly	GlyGlyHis
2,2,2-tet						
k_{H}		0.7		1.4	5.1×10^6	$^{a}0.5$
$k_{2\text{H}}$	6.0×10^2	1.2		2.3	1.2×10^5	
$k_{3\text{H}}$	3.3×10^2					1.1×10^2
EDTA						
k_{HEDTA}	7.5×10	0.49		0.17		
$k_{\text{H}_2\text{EDTA}}$	3.5×10^5	3.3×10^2	9.3×10^{-1}	2.7×10^2	3.1×10^3	1.7×10^2
k_{O}		7.5×10^{-2}	8.3×10^{-3}		0.12	7.5×10^{-4}
k_{H}		1.0×10^6	2.2×10^2		4.9×10^6	1.8×10^5

The dioxo(13)- and (15)aneN₄ similarly undergo substitution by trien, but at much slower rates. In the exchange reaction of EDTA with triglycine the poor nucleophile EDTA cannot expel the triglycine by the direct nucleophilic mechanism, but it can with the aid of the protons attached to it. A similar proton-assisted nucleophilic mechanism operates in the reaction with dioxo 2,3,2-tet, as evidenced by the fact that diprotonated H₂EDTA is a far more effective reactant than monoprotonated HEDTA. An inspection of the H₂EDTA reaction rates, k_{H_2EDTA} , for dioxo 2,3,2-tet to GlyGlyHis (Table III) shows that the dioxo(14)aneN₄ complex is inert to substitution. There appears to be an inverse relation between the stability constant K_{CuH_2L} and the displacement rates K_{H_2EDTA} . Thus the thermodynamic effects of cyclization of the oxo ligands and the ring size on the relative stability of the CuH₂L complexes are manifested in the ligand-replacement kinetics.

5. NICKEL(II) OXO POLYAMINE COMPLEXES

Nickel(II) forms yellow, low-spin (diamagnetic) complexes with dioxo(13)–(15) aneN₄ in aqueous solutions. This is a good illustration of the effect of the dioxo incorporation that enhances strong coplanarity of the N₄ donor atoms.³ Without the dioxo functions a high-spin state is in equilibrium with the low-spin Ni²⁺ and its proportion varies with the cavity size: 13:87 with (13)aneN₄, 29:71 with (14)aneN₄, and 99:1 with (15)aneN₄ at 25°C.^{23,24} The low-spin complex is a square planar form. The high-spin species with (14)- and (15)aneN₄ is a *trans* octahedral form having two coordinated water molecules in the axial positions or with smaller (13)aneN₄ is a folded *cis* octahedral form.²³

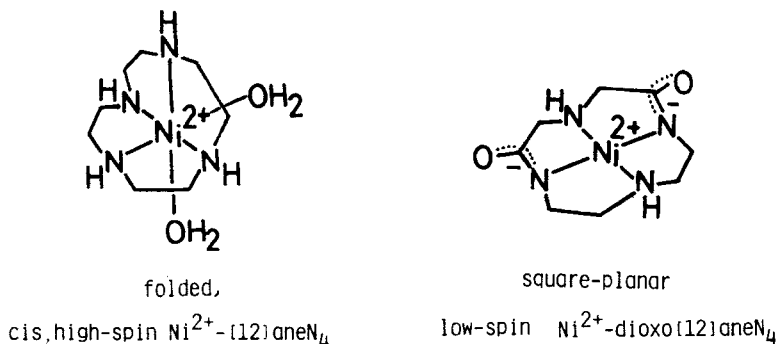


The normal length of the strain-free, high-spin Ni²⁺-N bond is 2.10 Å, while that of the low-spin Ni²⁺-N bond is 1.89 Å.¹⁵ The ideal M-N bond lengths for fitting into 13–15 membered N₄ are estimated to be 1.92, 2.07 and 2.22 Å, respectively. Then, the inplane nitrogens of larger macrocycles would have stronger interaction with the high-spin Ni²⁺, and those of the smaller macrocycles with the low-spin Ni²⁺. Thus, the low-spin form is predominant with the most ideally sized 13-membered macrocycle in the oxo-free system.²³ Moreover, the highest d-d absorption band $\nu(d-d) = 23530 \text{ cm}^{-1}$ occurs for the low-spin Ni²⁺ complex with (13)aneN₄, that reflects the largest Dq^{xy} among the (13)–(15)aneN₄.

Among the dioxo tetraamine system the 13-membered cavity fits the low-spin Ni²⁺ best.³ This notion results from the highest $\nu(d-d)$ 24300 cm⁻¹ (or shortest λ_{max} value) of d-d absorption spectra (see Table 2). This is in parallel with the oxo-free homologues. Interestingly, the low-spin Ni²⁺-N interaction is stronger for the dioxo(13)aneN₄, which we ascribe to the smaller (due to the imide anion resonance effect) and more

ideal cavity size for the low-spin Ni^{2+} bond length of 1.89 Å. It is of interest to note that the low-spin Ni^{2+} complex of a 13-membered N_4 containing conjugated two diimines is square planar with the Ni-N (trigonal) bond distance of 1.83 Å, shorter than the Ni-N (tetrahedral) length of 1.88 Å.²⁵ With Cu^{2+} having the longer Cu-N bond distance 2.03 Å,¹⁵ the dioxo(14)ane N_4 offers the best-fit cavity. Arrangement of the N_4 in-plane configuration by the dioxo(13)ane N_4 may cause minor strain in the linked three ethylenediamine ring conformation. On the other hand, the Ni^{2+} -dioxo(14)ane N_4 having alternative five- and six-membered chelates would encounter lesser resistance from the chelate conformation in placing the N_4 coplanar, although the coplanar N_4 cavity size is a little bigger for the low-spin Ni^{2+} . As a result the $K_{\text{CuH}_2\text{L}}$ value of the dioxo(13)ane N_4 complex is slightly smaller than that of the dioxo(14)ane N_4 complex. It is of interest to point out that the ligand field strength of the dioxo(13)ane N_4 complex is almost equivalent to that of the triply deprotonated tetraglycine complex taking a truly square-planar structure with an average Ni^{2+} -N (peptide) bond length of 1.85 Å.⁸

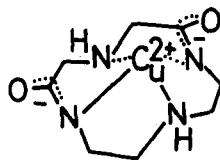
In contrast to the oxo-free macrocyclic homologues we see virtually no high-spin Ni^{2+} in the deprotonated dioxo tetraamine. Such an effect of the dioxo function is most illustrative in the square-planar complex of yellow low-spin Ni^{2+} with a 12-membered tetraamine.³ The (blue) Ni^{2+} complex of the parent (12)ane N_4 in aqueous solution (0.1 M NaClO_4) is more than 99% in the high-spin form (octahedral *cis* structure), which only under special conditions (higher temperature and ionic strength) is partially converted into the yellow, square-planar, low-spin form.²⁴ As far as the ring cavity size is concerned, the ideal M-N length for fitting into coplanar (12)ane N_4 (1.83 Å) is not prohibitively small for the low-spin Ni^{2+} .²⁵ In fact, the ligand field of the (12)ane N_4 complex is significantly high, as judged from $\nu(\text{d-d})$ of 23260 cm^{-1} .²³



However, the barrier to coplanar N_4 exhibited by the 12-membered macrocycle comprising four ethylenediamine chelates is so high due to the tremendous conformational strain and non-bonding repulsion, and overall (12)ane N_4 chooses the folded configuration with high-spin Ni^{2+} . The deprotonation at two amide groups (above pH 7.5) of dioxo(12)ane N_4 , which renders two N (sp^3) into N^- (sp^2 -type), greatly contributes to the stabilization of the square planar conformation of the 12-membered macrocycle that can enclose the low-spin Ni^{2+} . The much lower stability constant $K_{\text{NiH}_2\text{L}}$ (Table II) than for dioxo(13)-(15)ane N_4 indicates certain overall strain in forming the square-planar complex.

Copper(II) also forms a CuH_2L complex with dioxo(12)ane N_4 at pH > 7. Appreciable strain is manifested in the lowest d-d transition energy and the smallest $K_{\text{CuH}_2\text{L}}$ value among the relevant Cu^{2+} complexes in Table II. This is probably due to

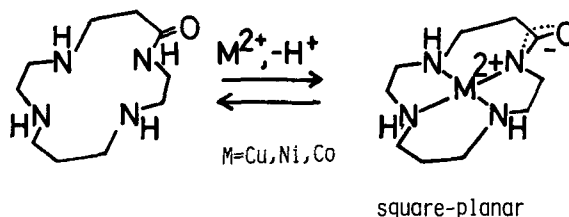
the small cavity size ($<1.83 \text{ \AA}$) relative to the Cu^{2+} -N bond length (2.03 \AA). As a result, Cu^{2+} would stay above the coplanar N_4 .



Cu^{2+} -dioxo(12)ane N_4

6. MONOOXO- AND TRIOXO TETRAAMINES

Monooxo tetraamines and trioxo tetraamines were synthesized and investigated as an extension of dioxo tetraamine ligands (Table IV). With monooxo(14)ane N_4 , the dissociation of an amide proton occurs at $\text{pH} > 4$ with simultaneous inclusion of Cu^{2+} ,²⁵ Ni^{2+} ,²⁵ and Co^{2+} .¹¹



The rigid square planar configuration of the singly deprotonated monooxo(14)ane N_4 is evident from the low-spin Ni^{2+} ($\mu_{\text{eff}} = 0$) complex in aqueous solution.²⁵

The pH titration curve for trioxo(14)ane N_4 initially showed dissociation of two amide protons in the presence of Cu^{2+} at $\text{pH} 6$ with the third amide hydrogen remaining undissociated.²⁵ The CuH_2L complex is blue ($\lambda_{\text{max}} 620 \text{ nm}$), in contrast to the pink complex ($\lambda_{\text{max}} 505\text{--}510 \text{ nm}$) of oxo-free to dioxo tetraamine homologues. Since the undissociated amide N would not interact with Cu^{2+} as strongly as other three N

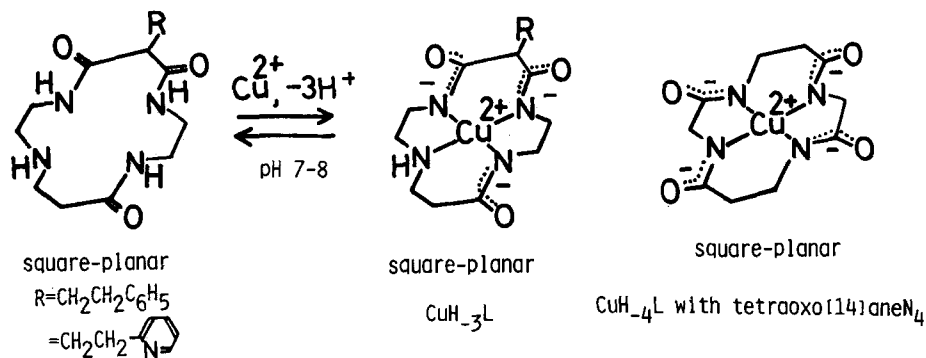
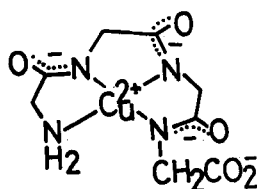


TABLE IV
Properties of 1:1 Metal Complexes at $I = 0.2 \text{ M}$ and 25°C (Cu^{2+}) or 35°C (Ni^{2+} and Co^{2+}).^a

Metal	Ligand (substituent)	Complex Formula	$\log K_{\text{MH}_{-1}}/M$	$\lambda_{\text{max}}/\text{nm}$ ($\epsilon/M^{-1} \text{ cm}^{-1}$)	E° for $\text{M}^{\text{II}}/\text{M}^{\text{I}}$ /V vs SCE	
Cu^{2+}	(14)aneN ₄	CuL		506 (80)	irreversible	
	(-CH ₂ CH ₂ -⊖)	CuL		510(105)	irreversible	
	monoox(14)aneN ₄	CuH ₋₁ L	(13.00) ^a	510 (80)	0.86	
	diox(14)ane	CuH ₋₂ L	1.00	505(100)	0.64	
	(-CH ₂ CH ₂ -⊖)	CuH ₋₂ L	-1.10	502 (95)	0.66	
	(-CH ₂ CH ₂ -⊖)	CuH ₋₃ L	-1.00	507(100)	0.66	
	triox(14)aneN ₄	CuH ₋₂ L	-9.24	620(130)	irreversible	
		CuH ₋₃ L		580(100)	0.43	
	(-CH ₂ CH ₂ -⊖)	CuH ₋₃ L	-16.34	490 (80)	0.49	
	(-CH ₂ CH ₂ -⊖)	CuH ₋₃ L	-16.20	490 (80)	0.49	
Ni^{2+}	tetraox(14)aneN ₄	CuH ₋₄		488 (54)	0.23	
	(14)aneN ₄	NiL		450 (70)	0.50	
	(-CH ₂ CH ₂ -⊖)	NiL		455 (55)	0.50	
	monoox(14)aneN ₄	NiH ₋₁ L	(4.00) ^a	488 (60)	irreversible	
	diox(14)aneN ₄	NiH ₋₂ L	-5.15	460(100)	0.81	
	(-CH ₂ CH ₂ -⊖)	NiH ₋₂ L	-6.30	455 (70)	0.88	
	(-CH ₂ CH ₂ -⊖)	NiH ₋₂ L	-5.94	457 (80)	0.86	

^aValue of $\log K_{\text{MH}_{-1}}/M$ ($= (\text{MH}_{-1})/(\text{H}^+)(\text{M})$) (L).

donors, the complex CuH_2L would not adopt a square-planar structure. At higher pH, 12–14, the blue solution turns to violet for which the spectrophotometric titration supports the dissociation of the third amide proton to CuH_3L . Curiously, three of the amide protons all at once dissociate at pH 7–8 with substituted trioxo(14)ane N_4 , where R is a phenylethyl and pyridylethyl group. The metal enclosure structure is identified by the d–d absorption (λ_{max} 490 nm) and ESR spectra similar to those for the CuH_2L complexes with dioxo tetraamines. Previously cyclic (gly- β -alanine) $_2$, abbreviated here as tetraoxo(14)ane N_4 , was reported to yield a quadruply deprotonated amide complex CuH_4L at pH >13,^{26,27} whose visible absorption spectrum (λ_{max} 488 nm) is very close to those (490 nm) of the CuH_3L with trioxo(14)ane N_4 . The highest $\nu(\text{d-d})$ of the CuH_3L among the 14-membered tetraamine family may indicate the most stringent constriction of the macrocyclic cavity, resulting in the strongest ligand field strength compared to those of CuL^{2+} (oxo-free), CuH_1L (monooxo), and CuH_2L (dioxo).



square-planar
 CuH_3L

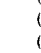
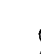
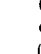
The ligand field strength of the triply deprotonated trioxo(14)ane N_4 is still higher than that (λ_{max} 515 nm) of the open-chain counterpart, triply deprotonated tetraglycine, which may be due to the “compression” effect of the tight macrocyclic structure and the inductive effect of the secondary nitrogen of the macrocycle.¹⁵

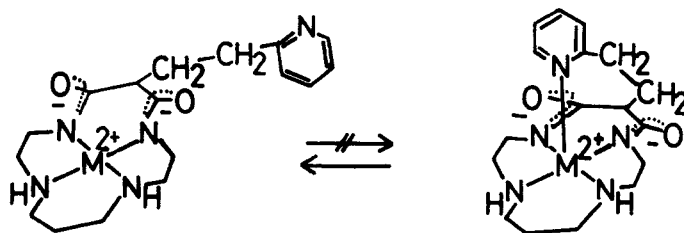
Nickel(II) and cobalt(II) fail to form complexes with trioxo(14)ane N_4 up to pH 12, indicating that these metal ions have insufficient M–N bond strength to make up for the dissociation of the three amide protons.

7. SUBSTITUTED OXO POLYAMINE MACROCYCLES

A molecular model suggests that a side-arm N donor attached to 14-membered tetraamines (e.g. $\text{R}=\text{CH}_2\text{CH}_2\text{-}$ or $(\text{CH}_2)_4\text{NH}_2$ of dioxo(14)ane N_4) can be axial ligand. However, such an axial coordination is hardly recognized in view of the similar values of $K_{\text{MH}_2\text{L}}$ (see Table V) and visible spectra (ESR spectra for Cu(II), too) as those for phenethyl (i.e. $\text{R}=\text{CH}_2\text{CH}_2\text{-}$) substituted homologues.²⁶ This is also the case for dioxo-free and trioxo(14)ane N_4 .²⁶ It is thought that the generally strong in-plane ligand fields produced by the 14-membered macrocyclic tetraamines cause strong tetragonal distortion and weaken the interaction with an intramolecular axial donor. It is also shown that the pyridyl-side arm does not alter the low-spin d^8 state ($\mu_{\text{eff}} = 0$) of the Ni^{2+} complexes. However, as mentioned in the following section, when such N donors are included within the macrocycle ring frame (e.g. (16)ane N_5 , dioxo(16)ane N_5 , pyrodioxo(16)ane N_5), the high-spin Ni^{2+} complexes are formed.

TABLE V
Complex Properties of Macrocyclic Oxopentaamines and Congeners.³⁰

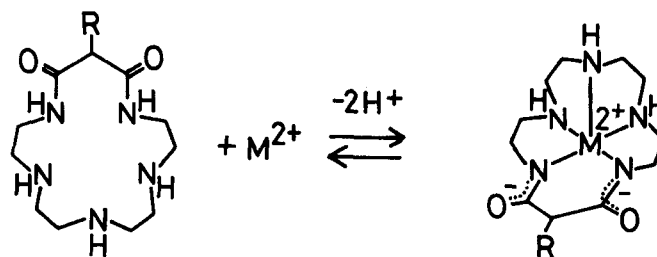
Metal	Ligand (Substituent)	Complex Formula	$\log K_{\text{MH}_2\text{L}}/M$	E° for $M^{\text{III/II}}$ (V vs SCE)
Ni^{2+}	(16)aneN ₅	NiL	($\log K_{\text{NiL}} = 17.72$)	0.66
	monooxo(16)aneN ₅	NiH ₋₁ L		0.46
	dioxo(16)aneN ₅	NiH ₋₂ L	-8.58	0.24
	(-H)	NiH ₋₂ L	-9.33	0.24
	(-CH ₃)	NiH ₋₂ L	-10.62	0.24
	(-CH ₂ - )	NiH ₋₂ L	-10.79	0.25
	(-CH ₂ - )	NiH ₋₂ L		
	(-CH ₂ CH ₂ - )	NiH ₋₂ L	-7.89	0.24
	(16)aneN ₄ ·Py	NiL		
	dioxo(16)aneN ₄ ·Py	NiH ₋₂ L	-12.72	0.62
(16)aneN ₄ ·S	NiL		0.77	
dioxo(16)aneN ₄ ·S	NiH ₋₂ L	-9.58	0.41	
(16)aneN ₄ ·(CH ₃)	NiL			
dioxo(16)aneN ₄ ·CH ₃	NiH ₋₂ L	-10.92	irreversible	
Cu^{2+}	dioxo(16)aneN ₅	CuH ₋₂ L	-5.54	0.68
	dioxo(16)aneN ₄ ·S	CuH ₋₂ L	-4.79	0.73
Co^{2+}	dioxo(16)aneN ₅	CoH ₋₂ L	-9.45	-0.63



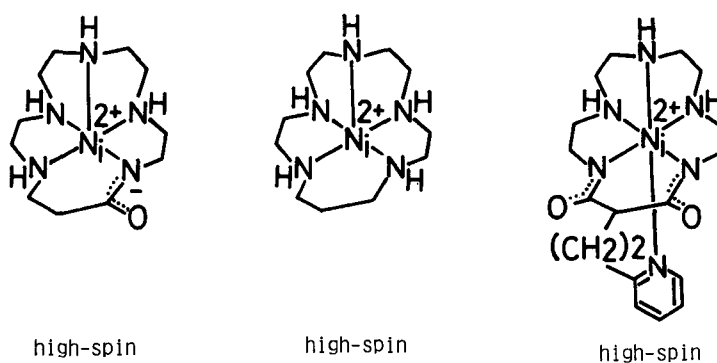
The pyridyl arm contributes to the net destabilization of MH_2L , of which magnitude tends to vary with the macrocyclic ring size. In the dioxo(14)aneN₄ complex with Cu^{2+} it exerts the greatest destabilization effect. In Cu^{2+} -dioxo(15)aneN₄ it has almost no effect. A parallel trend with the ring size is evident in Ni^{2+} complexes, where the dioxo(13)aneN₄ is subject to the greatest destabilization. The phenyl substituent brings about the same degree of destabilization as the pyridyl, suggesting that the steric blocking of the axial hydration is solely responsible for the complex destabilization.

8. MACROCYCLIC OXO PENTAAMINES AND CONGENERS

A macrocyclic dioxo pentaamine, dioxo(16)aneN₅, yields a 1:1 complex with Cu^{2+} and Ni^{2+} with concomitant double deprotonation, in which the five N donors of the ligand would encircle the M^{2+} ion in a square-pyramidal configuration only with the two imide anion donors occupying the basal positions due to the steric requirement.^{29,30} The pink Ni^{2+} complex displays three d-d absorption bands with the low extinction coefficient (ϵ 1-10) characteristic of octahedral high-spin species, as supported by the μ_{eff} value of 2.8.

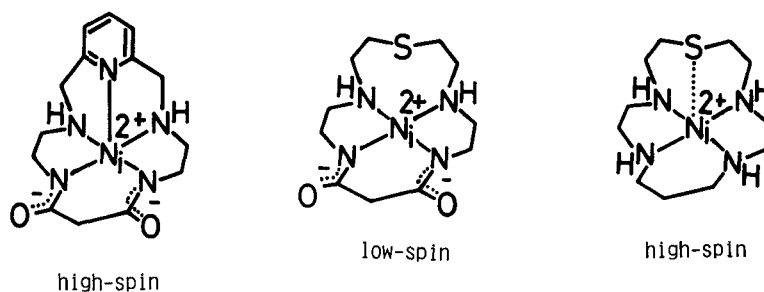


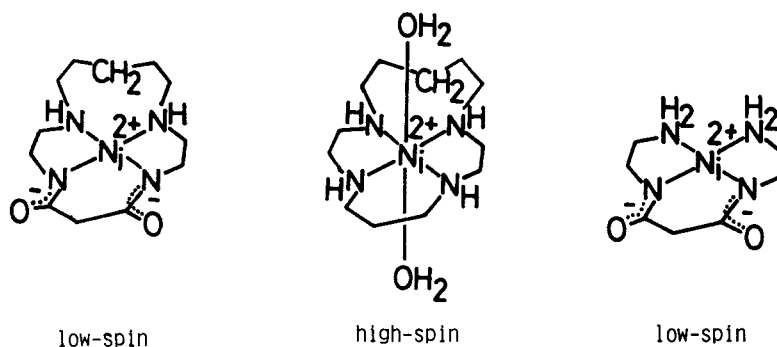
The monooxo(16)aneN₅ and oxo-free(16)aneN₅ offer a similar square-pyramidal N₅ ligand environment to high-spin Ni²⁺.



The pyridyl side-armed dioxo(16)aneN₅ also yields a high-spin Ni²⁺ complex, which is about ten times more stable than the dioxo(16)aneN₅ complex. This fact, along with failure of the reaction with O₂,³⁰ suggests the occupation of the 6th position by the intramolecular pyridyl donor.

The 5th axial donors incorporated within the 16-membered dioxo macrocyclic frames can produce either five coordinate, high-spin Ni²⁺ complexes of four coordinate, low-spin Ni²⁺ complexes. Thus, good σ donors such as amine and pyridine stabilize high-spin Ni²⁺, while a poor σ -donor, sulfur or a non σ -donor methylene group, stabilizes low-spin Ni²⁺. Moreover, the four coordinate, square-planar low-spin Ni²⁺ in the dioxo(16)aneN₄S converts to octahedral, high-spin Ni²⁺ in (16)aneN₄S if the dioxo functions are removed. These and the relevant complexes depicted below illustrate the opposite preference of imide anion donors (for low-spin Ni²⁺) and axial donors (for high-spin Ni²⁺) in the ligand fields.





It is noteworthy that the high-spin Ni^{2+} complexes of N_5 ligands dioxo(16)ane N_5 and 16(ane) N_5 , respectively, are less stable than the low-spin Ni^{2+} complexes of N_4 ligands dioxo(16)ane N_5 and (16)ane N_5 , respectively, are less stable than the low-spin Ni^{2+} complexes of N_4 homologous dioxo(14)ane N_4 and (14)ane N_4 (high-spin state in minor portion, see the preceding Chapter), despite the fact that the former group offers one more donor atom than the latter.²⁹ Evidently, the good-fit of the N_4 cavity to low-spin Ni^{2+} is of greater importance than the higher N_5 donor number effect on high-spin Ni^{2+} so far as the overall complex stability is concerned. Copper(II) also forms more stable complexes with the N_4 ligands than with the N_5 ligands.²⁹

9. OXYGENATION OF COBALT(II)-MACROCYCLIC OXOPOLYAMINE COMPLEXES

The interaction of molecular oxygen O_2 with cobalt(II) chelates has been extensively studied because of the relation to biological O_2 carriers³¹⁻³⁴ as well as the potential of the complexes to act as catalysts for the insertion of oxygen into organic substrates.³⁵ Polyamine ligands such as porphyrins,³⁶ salicylidenamines,³⁷ aliphatic polyamines,³⁸ amino acids or peptides,³⁹ or saturated^{40,41} and unsaturated macrocyclic tetraamines⁴² are known to promote the O_2 affinity of Co^{2+} . Except for rare cases, the O_2 adducts possess a μ -peroxo structure $\text{Co}^{3+}-\text{O}_2^{2-}-\text{Co}^{3+}$.

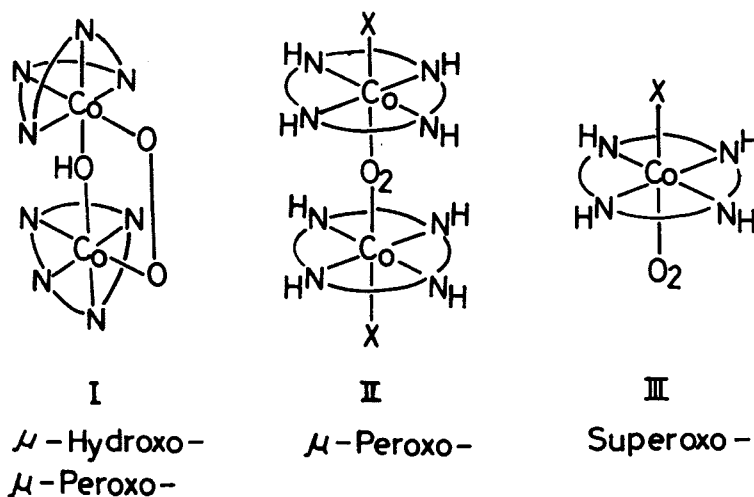
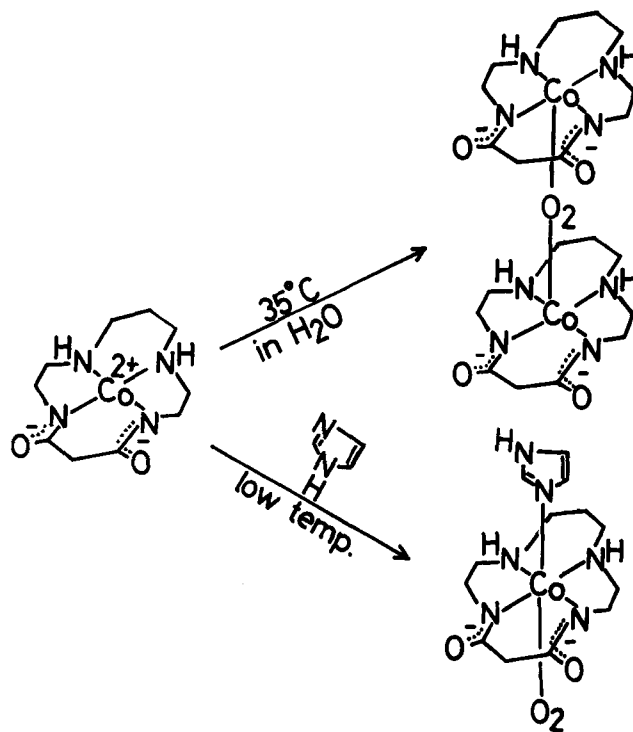


FIGURE 5 The O_2 adduct structures of Co^{2+} -macrocyclic tetraamines.

Our recent papers reported thermodynamic and kinetic data on O_2 affinities of Co(II) complexes with macrocyclic saturated polyamines (12)–(15)aneN₄,⁴³ (16)aneN₅ and its homologues.^{44–46} The ring size and donor ability are critical in determining the structure (Figure 5) and stability of the O_2 bonding. The smaller sized macrocycles (12)–⁴⁷ and (13)aneN₄,⁴⁸ which have a greater tendency to adopt folded conformations, yield the dibridging μ -peroxo- μ -hydroxo adducts I, while the larger (14)aneN₄, which was shown to take a square planar configuration with Co^{2+49} and Co^{3+50} produces the monobridging μ -peroxo adducts II. The (15)aneN₄ complex that is more disposed towards a trans configuration⁴⁸ was instantly autoxidized to a Co^{3+} species. The pentadentate macrocycles such as (16)aneN₅ increase the O_2 affinity both kinetically and thermodynamically with the μ -peroxo-type structure II.⁴⁴

When it comes to Co^{2+} -dioxo(13)aneN₄ (low-spin, $\log K_{CoH_2L} = -12.4$ at 35°C, $I = 0.2$ M) and -dioxo(14)aneN₄ (low-spin, $\log K_{CoH_2L} = -9.4$) both adopting possibly more rigid square-planar configurations than the dioxo-free homologues, the former undergoes immediate autoxidation to the Co^{3+} complex. In contrast, the latter yields the very stable μ -peroxo adduct II, the same formula as for (14)aneN₄.¹¹ Dioxo(15)aneN₄ and dioxo(12)aneN₄ fail to form the Co^{2+} complexes. The stronger σ donor effect of the dioxo(14)aneN₄ than of (14)aneN₄ is well manifested in a much greater O_2 affinity; $\log K_{O_2}$ ($= (CoL-O_2-CoL)/(CoL)^2(O_2)$) of 13.6 *vs.* 1.7 at 35°C, I 0.2 M.¹¹ The greater electron density at the central Co^{2+} ion means more back-donation to O_2 , resulting in a stronger Co– O_2 bond. The monooxo(14)aneN₄ can also greatly promote the O_2 uptake of Co^{2+} ; $\log K_{O_2}$ value of 8.6.¹¹ However, the potential for the $Co^{II/III}$ couple (polarographic $E_{1/2}$ value in borate buffer solution) does not appreciably vary with the oxo-incorporation and does not seem to directly correlate with the oxygenation behaviour in tetraamines: the (14)aneN₄ complex, -0.40 V *vs.* SCE; monooxo(14)aneN₄, -0.33 V; dioxo(14)aneN₄, -0.30 V. The $E_{1/2}$ value (-0.35 V) of the



dioxo(13)aneN₄ complex is similar to those for the 14-membered homologues, and yet it is immediately subject to autoxidation. On the other hand, there is a significant electrochemical difference for (16)aneN₅ ($E_{1/2} = -0.3$ V) and dioxo(16)aneN₅ (-0.63 V), which account for the stability of their O₂ adducts: the latter is immediately autoxidized to the Co³⁺ complex, while the former holds on as a stable μ -peroxo species ($\log K_{O_2} = 7.9$).

The occurrence of 1:1 O₂ adduct III was indicated by an ESR study in the presence of imidazole and at low temperature <-15°C.⁵¹ The formation of the 1:1 and 2:1 O₂ complexes¹² depending on temperature correlates well with the porphyrin system. The interesting reactivity of Co²⁺-dioxo(14)aneN₄ complexes with O₂ certainly merits further study for development of useful O₂ carriers.

10. STABILIZATION OF COPPER(III) AND NICKEL(III) BY MACROCYCLIC OXO POLYAMINES

Recently it was found that the uncommon oxidation states of Cu³⁺ (ref. 52, 53) and Ni³⁺ (ref. 54) can be stabilized by coordination to deprotonated amide nitrogen donors. The triply deprotonated tetraglycine complex of Cu³⁺ was characterized in aqueous solution.⁵⁵ Its formation was initially observed during the studies of the reaction of oxygen with Cu²⁺-tetraglycine, and subsequently its stoichiometry and reduction potential were determined.⁵⁶ The electrode potentials for Cu^{III/II},⁵⁷ and Ni^{III/II}-peptide complexes⁵⁸ have since been determined to seek factors for thermodynamic stabilization of M³⁺ relative to M²⁺. The kinetic stability of Cu³⁺-peptide complexes has also been studied.⁵⁹ Recently, a crystal structure of a Cu³⁺-tripeptide complex has been reported.⁶⁰ Nickel(III) complexes with macrocyclic tetraamines are known to be stable in aprotic solvents.⁶¹ Recently, Ni³⁺-(14)aneN₄ was prepared and characterized in aqueous solution⁶² and in crystal.⁶³ However, Cu³⁺-(14)aneN₄ was too unstable to be identified.⁶⁴

We have discovered thermodynamic stabilization of Cu³⁺ and Ni³⁺ in aqueous solutions using our macrocyclic oxo polyamines with varying size.⁴ Moreover, M³⁺ in macrocyclic complexes are found to be kinetically more stable than M³⁺ in open-chain peptide complexes.³ The electrochemical oxidation potentials for M^{III/II} were successfully determined by cyclic voltammetry (Figure 6), the potentials which are contained in Table II, IV, and V. The electrochemically or chemically (by IrCl₆²⁻) generated Cu³⁺ and Ni³⁺ in oxo polyamine complexes generally show strong brown C-T spectra similar to those for peptide complexes. The ESR spectra also supplied evidence for a low-spin d⁸ (diamagnetic) Cu³⁺ and a low-spin d⁷ ($S = 1/2$) Ni³⁺ in the oxidized macrocyclic complexes.²⁶

The overall oxidation potential of the macrocyclic M²⁺ complexes measures the thermodynamic stabilization of M³⁺ relative to M²⁺ and is a composite function of the size of the aperture, number of amide functional groups, type of appended substituents and the number and type of donor atoms. With a broad family of macrocyclic complexes that can stabilize M³⁺ in aqueous solutions at hand, the observed pattern of the oxidation behavior can be meaningfully correlated with those properties characteristic to macrocyclic polyamine complexes.

11. VARIATION OF OXIDATION PROPERTIES WITH MACROCYCLIC PARAMETERS

11.1 Effects of the Aperture Size on E°

In a progression from dioxo(13)aneN₄ to dioxo(16)aneN₄ with the aperture size being the sole varying factor the low-spin d⁸ ($S=0$) Ni²⁺ \rightarrow low-spin d⁷ ($S=1/2$) Ni³⁺ process

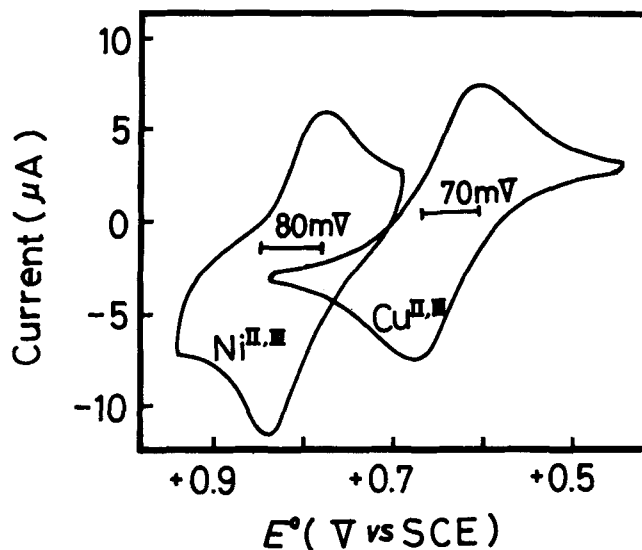
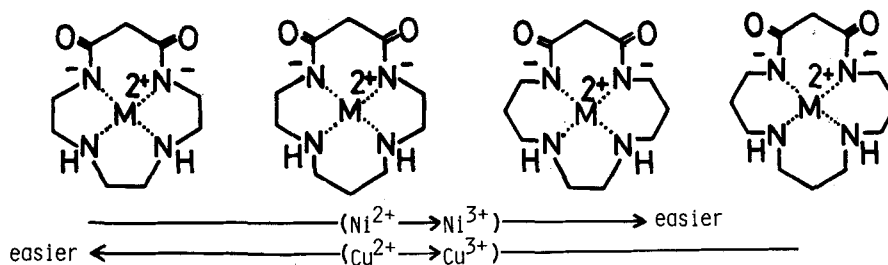


FIGURE 6 Cyclic voltammograms of Cu^{II} - and Ni^{II} -complexes with doubly deprotonated dioxo(14)ane N_4 at $(\text{MH}_2\text{L}) = 1 \text{ mM}$ ($\text{M} = \text{mol dm}^{-3}$), $0.5 \text{ M Na}_2\text{SO}_4$, $\text{pH} = 9$ (unbuffered), and 25°C ; Scan rate 50 mV s^{-1} with glassy carbon electrode.

occurs with greater ease.³ (An extending dioxo(16)ane N_4 gave an irreversible voltammogram and its E° could not be determined.) On the other hand, the d^9 ($S=1/2$) $\text{Cu}(\text{II}) \rightarrow$ low-spin d^8 ($S=0$) $\text{Cu}(\text{III})$ process occurs with progressive difficulty as the ring size increases.³



The reverse ordering of potentials with Ni and Cu is of interest and may be attributed to the loss or gain in the equatorial ligand field strength and in the axial solvation accompanying the change of the M-N bond lengths and the electronic states in the transition from M^{2+} to M^{3+} .

It has been established by crystal structure analysis of a peptide complex⁶⁰ that Cu^{3+} -ligand bond lengths are $0.12\text{--}0.17 \text{ \AA}$ shorter than the corresponding Cu^{2+} bonds and $0.02\text{--}0.04 \text{ \AA}$ shorter than the corresponding low-spin Ni^{2+} bonds. Accordingly, one expects the best fit size of macrocycle to shift from the 14-membered cavity for Cu^{2+} to the smaller sized 13-membered cavity for Cu^{3+} . It then follows that, the dioxo(13)ane N_4 ligand field should most stabilize Cu^{3+} and the dioxo(16)ane N_4 least stabilize it, as in fact is shown by the relative E° values. Upon the electronic configurational change from d^9 Cu^{2+} to the low-spin d^8 Cu^{3+} , one would expect the loss of axial solvation, which was proved to be true by the study of E° values as a functions of solvent polarity and temperature.²⁶ The desolvation should be more favourable as the increase in tetragonal distortion by the smaller macrocyclic ligand fields.

Despite the higher oxidation state, the low-spin d^7 Ni^{3+} would have longer bond distance with N(amino), e.g. 1.97 Å in $Ni^{3+}nd(14)aneN_4Cl_2$,⁶³ than the low-spin d^8 Ni^{2+} (1.89 Å)¹⁵. This is not unexpected in reference to the low-spin d^7 $Co^{3+}-N$ (1.98 Å),⁴⁹ the low-spin d^6 $Co^{3+}-N$ (~2 Å),⁵ and the high-spin d^8 Ni^{2+} (2.2 Å) (which best fits to the largest 15-membered macrocyclic cavity among (13)-(15)ane N_4).⁶⁵ Then, it is readily understood that the Ni^{2+} in the tight-fit dioxo(13)ane N_4 cavity is most difficult to oxidize to Ni^{3+} . On the other hand, the loosely-fit dioxo(15)ane N_4 may be most favorable for the nickel oxidation. Moreover, the low-spin d^7 Ni^{3+} metal ion is more likely to have axial hydration that is expected to be more favorable with a larger macrocyclic size due to the weaker in-plane ligand fields.

Among all of the tetraamine macrocycles the smallest planar macrocycle, dioxo(12)ane N_4 , most favors the oxidation to Cu^{3+} . Its E° value of 0.42 V is in the range for the tetraglycine complex (0.38 V).

11.2 Effect of Imide Anion Donor on E°

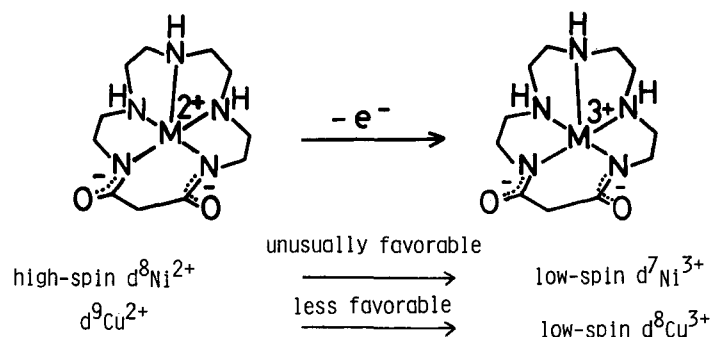
The deprotonated peptide nitrogen is a strong in-plane donor and is a stronger σ donor than amine.⁹ Replacement of an amine by a deprotonated amide lowers E° by 0.15 V in Cu^{2+} -peptide complexes.⁵⁷ Hence, the more imide donors, the more stable the Cu^{3+} state is. A similar trend was found with the 14-membered tetraamines; E° value being 0.86 V for singly deprotonated monooxo, 0.64 V for doubly deprotonated dioxo, and 0.43 V for triply deprotonated trioxo tetraamine. Accordingly the replacement of amines by imide anions in the 14-membered tetraamines stabilizes the Cu^{3+} state as additively as in the peptides. Interestingly, quadruply deprotonated tetraoxo(14)ane N_4 , although it is not strictly homologous to other oxo tetraamines, has an E° value of 0.23 V (vs. SCE)²⁸ which is 0.20 V lower than the trioxo(14)ane N_4 and stays in the same line of additivity.

With nickel complexes of peptides, similar stabilization by an imide anion also occurs,⁶⁶ though this effect is not as great (0.02-0.06 V) as with the copper complexes. A similar trend is seen with 15-membered macrocycle; (15)ane N_4 complex (0.77 V) vs. dioxo(15)ane N_4 (0.62 V). However, the opposite trend is seen with 14-membered ligands; (14)ane N_4 (0.50 V) vs. dioxo(14)ane N_4 (0.80 V). The monooxo(14)ane N_4 gives only an irreversible voltammogram. We ascribe this unusual fact to an unusually low E° value of the oxo-free (14)ane N_4 , owing to the great stabilization of Ni^{2+} by the strong axial interaction of SO_4^{2-} that is added as a supporting electrolyte. As a supporting evidence the use of the weaker coordinating anion ClO_4^- (0.1 M) in place of SO_4^{2-} (0.5 M) was found to raise the E° value of Ni^{2+} -(14)ane N_4 to 0.68 V.

11.3 Square Pyramidal N_5 Coordination Environments for Stability of M^{3+} .

The most interesting finding with the dioxo polyamine series was the dramatic drop of E° values of the $Ni^{III/II}$ couple when the fifth donor atom is incorporated into the macrocyclic rings; from +0.80 V with dioxo(14)ane N_4 to +0.24 V with dioxo(16)ane N_5 .²⁹ This is remarkable, since in any other ligand system such as the peptides (e.g. 0.71 V of GlyGlyHis vs. 0.70 V of GlyGlyHisGly),⁵⁷ macrocyclic tetraamine rings (e.g. 0.81 V of dioxo(14)ane N_4 vs. 0.86 V of pyridyl-tail dioxo(14)ane N_4)²⁶ and oxo-free macrocycles (e.g. 0.50 V of (14)ane N_4 vs. 0.66 V of (16)ane N_5),²⁹ E° values for $Ni^{III/II}$ couples are insensitive to the attachment of an additional axial donor. Moreover, the 0.24 V of dioxo(16)ane N_5 is exceptionally low among the reported $Ni^{III/II}$ redox values of the relevant polyamines and peptide complexes in aqueous solution. The ability of the imide anion to lower the E° value in the high-spin Ni^{2+} -16-membered N_5 is evident; 0.66 V for oxo-free, 0.46 V for monooxo, and 0.24 V for dioxo. Interestingly, the ease of oxidation of Cu^{2+} to Cu^{3+} is almost unaffected by going from dioxo(14)ane N_4 (0.64 V) to dioxo(16)ane N_5 (0.68 V). Further, the fact that the $Ni^{III/II}$ potential (+0.24 V) is much

lower than the corresponding $\text{Cu}^{\text{III/II}}$ potential (+0.68 V) with the same ligand has no precedence in peptide systems. The opposite is generally true,⁶⁵ as is the case with the dioxotetraamine macrocyclic systems. The amide-deprotonated peptides and dioxo-tetraamines commonly complex with low-spin Ni^{2+} , but not with high-spin Ni^{2+} (except for $\text{Ni}(\text{H}_{-1}\text{GlyGly})_2$).⁹ Thus, the disposition of the high-spin Ni^{2+} in the larger macrocycle should be also important to determine the E° values. These facts taken together well illustrate how the square pyramidal N_5 coordination environments formed by the doubly deprotonated dioxo(16)ane N_5 are effective for the $d^8 \text{Ni}^{2+} \rightarrow d^7 \text{Ni}^{3+}$ process.



11.4 Effect of Axial Donor in the 16-Membered Macrocyclic Backbone

The axial donor atoms generally help stabilize Ni^{3+} .³⁹ The relative ease of oxidation of Ni^{2+} to Ni^{3+} with amine (0.24 V) and thioether (0.41 V) reflects the relative σ -donor strength of N and S. The parallel order is seen for dioxo-free polyamines: amine (0.66 V) and thioether (0.77 V). The larger E° value of 0.62 V with pyridyl N donor compared to those with N and S may be attributed to the negative effect of π -back bonding. It is concluded that dioxo(16)ane N_5 probably is the most ideal structure for stabilization of Ni^{3+} .

SUMMARY AND CONCLUDING REMARKS

Replacement of amine with amide groups in macrocyclic polyamines yields a novel and unique ligand system that is a hybrid of macrocyclic polyamines and oligopeptides. Moreover, they are gifted with some distinctive properties that are not attached to either of the parent compounds. The disclosed characteristics of oxo polyamines and their metal complexes in reference to oxo-free polyamines and peptides may be summarized as follows:

1) Macrocyclic oxo tetraamines in general are more selective than oxo-free systems in interaction with metal ions. Only those metal ions Cu^{2+} , Ni^{2+} , Co^{2+} , and Pd^{2+} that can displace the protons of peptide nitrogens go into the macrocyclic cavities with concomitant dissociation of the amide protons (that occurs normally at lower pH than the dissociation of peptide hydrogens), yielding stable square-planar complexes MH_4L .

2) The rigid coplanarity and strong in-plane ligand fields of the deprotonated oxo tetraamine macrocycles (12–15-membered) are well demonstrated in the complexation of only the low-spin form of Ni^{2+} . On the other hand, the oxo-free homologous (12)–(15)ane N_4 yield both the low-spin and high-spin Ni^{2+} complexes. Of the homologous dioxo(13)–(15)ane N_4 , the dioxo(13)ane N_4 having the smallest cavity fits best the low-spin Ni^{2+} and produces a higher ligand field than the (13)ane N_4 . The overall complex stability is highest with the dioxo(14)ane N_4 .

3) Due to the strong coplanarity caused by the two conjugated imide anions, the dioxo(12)aneN₄ yields the square-planar, low-spin Ni²⁺ complex. On the other hand, (12)aneN₄ cannot take but a folded *cis*-configuration with high-spin Ni²⁺.

4) The ionization of the two amide hydrogens occurs simultaneously (to CuH₂L) upon interaction of Cu²⁺, for dioxotetraamines, whereas for peptides (e.g. triglycine) the ionization occurs stepwise (to CuL, CuH₁L). The cooperative proton dissociation from the two amides of a macrocycle is due to the proximity effect, for which the restricted conformation of macrocyclic structures is responsible. The stability of the doubly deprotonated dioxotetraamines CuH₂L varies with the ring size: dioxo(14)aneN₄ fits best to Cu²⁺ and hence yields the most stable complex, which is more stable than any of the doubly deprotonated tripeptide complexes reported in the literature.

5) The thermodynamic stability of the macrocyclic system should be derived from the unusually slow dissociation (or substitution) rates.

6) Cobalt(II) interacts only with the size-fit dioxo(13)- and (14)aneN₄ to give the low-spin CoH₂L. The dioxo(14)aneN₄ complex reacts with O₂ to form a more stable 2:1 O₂ adduct than the (14)aneN₄ complex.

7) The oxo functions in square-pyramidal macrocyclic pentadentate complexes are placed at the equatorial position. The amide deprotonated tri- and tetrapeptides complex only with low-spin Ni²⁺, but not with high-spin Ni²⁺. On the other hand, stable, high-spin Ni²⁺ complexes possessing deprotonated amides can be obtained with macrocyclic pentadentate ligands.

8) Just like peptide ligands, the oxo polyamines can stabilize Cu³⁺ and Ni³⁺. Replacement of an imine by an imide anion additively lowers the redox potential E° for M^{III/II} couples. The macrocyclic ring size has a profound effect on the E° values. The smallest dioxo(12)aneN₄ most stabilizes the M³⁺ state in the tetraamine system. The Cu³⁺ and Ni³⁺ macrocyclic complexes in general are kinetically more stable and hence their lives are longer than peptide complexes. Accordingly, along with the versatility of structural modification, the macrocyclic oxo polyamines offer a suitable system for the basic study of Cu³⁺ and Ni³⁺ that are currently attracting considerable attention chemically⁶⁷ and biochemically.⁶⁸

9) The incorporation of a fifth axial donor in the dioxopolyamine 16-membered macrocyclic frame produces the high-spin, square-pyramidal Ni²⁺ complexes. Their E° values are lower (indicating more favourable formation of Ni³⁺) than those of the square-planar, low-spin Ni²⁺-dioxotetraamine complexes. Most notably, the Ni²⁺ complex of dioxo(16)aneN₅ exhibits the lowest E° value of +0.24 V (vs SCE) among all of the oxo polyamine complexes with Ni and Cu. The novel reactivity of the Ni²⁺-dioxo(16)aneN₅ with O₂^{29,30} is certainly derived from its low E° value and the high-spin Ni state.

The fundamental knowledge of macrocyclic oxo complexes is no less useful than the application in the oxygenase model⁶⁹ and the superoxide dismutase model.^{70,71} In the future we will find a wider scope of chemical and biochemical applications in such fields as selective metal ion transport, stabilization of unusual oxidation states of other metal ions (e.g. Ag³⁺),⁷² redox enzyme models, or drugs based on these chemical reactivities.⁷³

REFERENCES

1. M. Kodama and E. Kimura, *J. Chem. Soc., Dalton Trans.*, 325 (1979).
2. M. Kodama, T. Yatsunami and E. Kimura, *J. Chem. Soc., Dalton Trans.*, 1783 (1979).
3. M. Kodama and E. Kimura, *J. Chem. Soc., Dalton Trans.*, 694 (1981).

4. *Coordination Chemistry of Macrocyclic Compounds*, ed. G.A. Melson, Plenum Press, New York and London, 1979.
5. E. Kimura and M. Kodama, *Yuki Gosei Kagaku* (Organic Synthetic Chemistry), **35**, 632 (1977).
6. M. Kodama, E. Kimura and S. Yamaguchi, *J. Chem. Soc., Dalton Trans.*, 2536 (1980).
7. H. Fujioka, E. Kimura and M. Kodama, *Chem. Lett.*, 737 (1982).
8. H.C. Freeman, *Advances in Protein Chemistry* (Academic Press, New York, 1967), Vol 22, pp. 258-424.
9. D.W. Margerum and G.R. Dukes, *Metal Ions in Biological Systems* (Marcell Dekker, New York, 1974), Vol 1, pp. 158-213.
10. I. Tabushi, Y. Tanigushi and H. Kato, *Tetrahedron Letters*, 1049 (1977).
11. R. Machida, E. Kimura and M. Kodama, *Inorg. Chem.*, **22**, 2055 (1983).
12. H. Ojima and K. Yamada, *Nippon Kagaku Zasshi*, **91**, 49 (1970).
13. P.A. Tasker and L. Sklar, *Cryst. Mol. Struct.*, **5**, 329 (1975).
14. L. Fabbri, C. Mealli and P. Paoletti, *J. Chem. Res. (s)*, 170 (1979).
15. V.J. Thom, J.C.A. Boeyens, G.J. McDougall and R.D. Hancock, *J. Am. Chem. Soc.*, **106**, 3198 (1984).
16. F.P. Hinz and D.W. Margerum, *J. Am. Chem. Soc.*, **96**, 4993 (1974); *Inorg. Chem.*, **13**, 2941 (1974).
17. M. Kodama and E. Kimura, *J. Chem. Soc. Chem. Comm.*, 896 (1975); *J. Chem. Soc., Dalton Trans.*, 1720 (1976).
18. M. Kodama and E. Kimura, *J. Chem. Soc., Dalton Trans.*, 2341 (1976).
19. M. Kodama and E. Kimura, *J. Chem. Soc., Dalton Trans.*, 1473 (1977).
20. M. Kodama and E. Kimura, *J. Chem. Soc., Dalton Trans.*, 2269 (1977).
21. J.P. Laussac and B. Sarkar, *J. Biol. Chem.*, **255**, 7563 (1980).
22. J.F. Wong, J.C. Cooper and D.W. Margerum, *J. Am. Chem. Soc.*, **98**, 7268 (1976).
23. L. Fabbri, *J. Chem. Soc., Dalton Trans.*, 1857 (1979).
24. L. Fabbri, M. Micrefloni and P. Paoletti, *Inorg. Chem.*, **19**, 535 (1980).
25. M.F. Richardson and R.E. Sievers, *J. Am. Chem. Soc.*, **94**, 4134 (1972).
26. E. Kimura, T. Koike, R. Machida, R. Nagai and M. Kodama, *Inorg. Chem.*, **23**, 4181 (1984).
27. J.S. Rybka and D.W. Margerum, *Inorg. Chem.*, **19**, 3068 (1980).
28. J.S. Rybka and D.W. Margerum, *Inorg. Chem.*, **20**, 1453 (1981).
29. E. Kimura, A. Sakonaka, R. Machida and M. Kodama, *J. Am. Chem. Soc.*, **104**, 4255 (1982).
30. E. Kimura, R. Machida and M. Kodama, *J. Am. Chem. Soc.*, **106**, 5497 (1984).
31. R.C. Wilkins, *Adv. Chem. Ser.*, No. 100, 111 (1971).
32. F. Basolo, B.M. Hoffman and A. Ibers, *Acc. Chem. Res.*, **8**, 384 (1975).
33. A.E. Martell and G. McLendon, *Coord. Chem. Rev.*, **19**, 1 (1976).
34. R.D. Jones, D.A. Summerville and F. Basolo, *Chem. Rev.*, **79**, 139 (1979).
35. A. Nishinaga, H. Tomita, K. Nishizawa and I. Matsuura, *J. Chem. Soc., Dalton Trans.*, 1477 (1981).
36. B.R. James, "The Porphyrins", D. Dolphin, Ed. (Academic Press, New York, 1978) Vol 6.
37. A. Puxeddu and G. Costa, *J. Chem. Soc., Dalton Trans.*, 1115 (1981).
38. S.A. Bedell, J.H. Timmons, A.E. Martell and I. Murase, *Inorg. Chem.*, **21**, 874 (1982).
39. W.R. Harris, G. McLendon and A.E. Martell, *J. Am. Chem. Soc.*, **98**, 8378 (1976).
40. B. Bosnick, C.K. Poon and M.L. Tobe, *Inorg. Chem.*, **5**, 1514 (1966).
41. G. McLendon and M. Mason, *Inorg. Chem.*, **17**, 362 (1978).
42. D.H. Busch and J.C. Stevens, *J. Am. Chem. Soc.*, **102**, 3285 (1980).
43. M. Kodama and E. Kimura, *J. Chem. Soc., Dalton Trans.*, 327 (1980).
44. M. Kodama and E. Kimura, *Inorg. Chem.*, **19**, 1871 (1980).
45. E. Kimura, M. Kodama, R. Machida and K. Ishizu, *Inorg. Chem.*, **21**, 595 (1982).
46. M. Kodama, T. Koike, N. Hoshiga, R. Machida and E. Kimura, *J. Chem. Soc., Dalton Trans.*, 673 (1984).
47. Y. Iitaka, M. Shina, E. Kimura, *Inorg. Chem.*, **13**, 2886 (1974).
48. Y. Hung, L.Y. Martin, S.C. Jackels, A.M. Tait and D.H. Busch, *J. Am. Chem. Soc.*, **99**, 4029 (1977).
49. J.F. Endicott, J. Lillie, J.M. Kiszaj, B.S. Ramaswamy, W.G. Schmonsees, M.G. Simic, M.D. Glick and D.P. Rillema, *J. Am. Chem. Soc.*, **99**, 429 (1977).
50. C.K. Poon and M.L. Tobe, *J. Chem. Soc.*, A, 2069 (1967); 1549 (1968).
51. K. Ishizu, J. Hirai, M. Kodama and E. Kimura, *Chem. Lett.*, 1045 (1979).
52. J.J. Bour, P.J.M.W. Birker and J.J. Steggerda, *Inorg. Chem.*, **10**, 1202 (1971).
53. W.E. Keyes, J.B.R. Dunn and T.M. Loehr, *J. Am. Chem. Soc.*, **99**, 4527 (1977).
54. F.P. Bossu and D.W. Margerum, *J. Am. Chem. Soc.*, **98**, 4004 (1976).
55. G.L. Burce, E.B. Paniago and D.W. Margerum, *J. Chem. Soc. Chem. Comm.*, 261 (1975).
56. D.W. Margerum, K.L. Chellappa, F.P. Bossu and G.L. Burce, *J. Am. Chem. Soc.*, **97**, 6894 (1975).
57. F.P. Bossu, K.L. Chellappa and D.W. Margerum, *J. Am. Chem. Soc.*, **99**, 2195 (1977).
58. J.L. Kurtz, G.L. Burce and D.W. Margerum, *Inorg. Chem.*, **17**, 2454 (1978).
59. J.S. Rybka, J.L. Kurtz, T.A. Neubecker and D.W. Margerum, *Inorg. Chem.*, **19**, 2791 (1980).
60. L.L. Diaddario, W.R. Robinson and D.W. Margerum, *Inorg. Chem.*, **22**, 1021 (1983).
61. F.V. Lovecchio, E.S. Gore and D.H. Busch, *J. Am. Chem. Soc.*, **96**, 3109 (1974).
62. E. Zeigerson, G. Ginzburg, M. Schwartz, Z. Luz and D. Meyerstein, *J. Chem. Soc., Chem. Comm.*, 241 (1979).

63. T. Ito, K. Sugimoto, K. Toriumi and H. Ito, *Chem. Lett.*, 1477 (1981).
64. E. Zeigerson, G. Ginzburg, D. Meyerstein and L.J. Kirschenbaum, *J. Chem. Soc., Dalton Trans.*, 1243 (1980).
65. L.Y. Martin, C.R. Sperati and D.H. Busch, *J. Am. Chem. Soc.*, **99**, 2968 (1977).
66. F.P. Bossu and D.W. Margerum, *Inorg. Chem.*, **16**, 1210 (1977).
67. M. Virekananda and P.T. Prumal, *Tetrahed. Lett.*, **22**, 2605 (1981).
68. N. Kojima, J.A. Fox, R.P. Hausinger, L. Daniels, W.H. Orme-Johnson and C. Walsh, *Proc. Natl. Acad. Sci. USA*, **80**, 378 (1983).
69. E. Kimura and R. Machida, *J. Chem. Soc., Chem. Comm.*, 499 (1984).
70. E. Kimura, A. Sakonaka and M. Nakamoto, *Biochim. Biophys. Acta*, **678**, 172 (1981).
71. E. Kimura, A. Yatsunami, A. Watanabe, R. Machida, T. Koike, H. Fujioka, Y. Kuramoto, M. Sumomogi, K. Kunimitsu and A. Yamashita, *Biochim. Biophys. Acta*, **745**, 37 (1983).
72. L.J. Kirshenbaum and J.D. Rush, *J. Am. Chem. Soc.*, **106**, 1003 (1984).
73. The crystal structure of NF_3^+ -dioxo(16)ane N_3 complex has been reported after this manuscript was submitted: Y. Kushi, R. Machida and E. Kimura, *J. Chem. Soc. Chem. Comm.*, 216 (1985).